REPORT UMR - 27

PROGRESS REPORT NO. 3

AAF CONTRACT W33-038 ac 2100

PERIOD 3 1 November, 1948 to 1 January, 1949

TABLE OF CONTENTS

		Page No.
I.	List of Figures	iii
II.	Definition of Terms and Symbols	iv
III.	Summary of Past Work (Period I - 1 July to 1 September, 1948) (Period II - 1 September to 1 November, 1948)	1
IV.	Summary of Period 3 (1 November, 1948 to 1 January, 1949)	2
V.	Progress	3
	Blowoff Velocity	3
	Large Scale Combustion Chamber	13
	Temperature & Pressure Effects on Combustion Processes	13
	Flow Associated with the V-Flame	21
	Detonation	27
	Blow Down Equipment	27
VI.	Astivities Visited	31
VII.	Program for Next Period	32
	References	33
	Distribution	34

I. List of Figures

Fig. No.	Title	Page
1 thru 8	Photographs showing the effect of a cylindrical rod inserted downstream of a spherical flameholder	5 thru 12
9	Flameholder Assembly for Large Scale Combustion Chamber	14
10	Schematic Drawing of Test Set-up to study temperature and pressure effects on combustion processes	16
11	Photograph of normal flame	18
12	Flame speed versus fuel-air ratio	19
13	Distance between burner lip and bottom of flame cone versus combustion box pressure	20
14	Unconfined V-flame	21
15	Coordinate System	24
16	Velocity Profile	24
17	Coordinate System	25
18	Confined V-flame	26
19	Heat Exchanger Bed Dimensions (Graph)	29
20	Bed & Air Temperature vs. Bed Depth (Graph)	30

II. DEFINITION OF TERMS AND SYMBOLS

A_c = Surface area of the flame cone

A = Area

P = Pressure

Q = Volumetric rate of flow of the unburned mixture

V = Velocity

V_f = The normal flame speed relative to the unburned mixture

d = One half combustion chamber width

h = Enthalpy

u = Velocity component parallel to x axis

v = Velocity component parallel to y axis

ϕ = Velocity potential

ψ = Stream function

α = Angle between flame front and streamline

∂_q = Quenching distance

Q' = As defined in Figure 17

P_c = Combustion Box Pressure

f/A = Fuel - Air Ratio

Numerical subscripts on the above terms refer to measurements made at the points indicated in Fig. 14.

Pilot Flame = See Photograph No. 8, page 6
Also Page 7 of Reference 1.

III. Summary of Past Work

Blowoff Velocities

Blowoff data for spherical flame holders in a 5/8 inch jet were collected. These tests indicated a need for blowoff equipment capable of 400 ft. per second in a two inch nozzle. The system was designed and largely assembled.

Large Scale Combustion Chamber

The burner assembly was successfully operated several times with the aid of a hydrogen pilot flame.

A method of combustion chamber evaluation based on momentum considerations has been worked out which does not necessitate high temperature measurements.

Temperature and Pressure Effects on Combustion Processes

The small scale equipment to study the effect of pressure on combustion was designed and assembled. Preliminary tests indicated the desirability of some minor alterations in the system. These alterations were incorporated.

Flow Associated with a V-Flame

Conformal transformations were attempted on the V-Flame.

Detonation

Calculation and design of a shock tube to study detonation were made.

Blow Down Equipment

The design study of the blow down equipment was continued.

IV. Summary of Period 3

Blowoff Velocity

The construction of the blowoff equipment capable of 400 ft. per second was completed and the flow instruments calibrated. Exploratory tests on flame holders which were operating at near blowoff velocities indicated that combustion is improved by the insertion of a second flame holder at some definite distance downstream of the first holder.

Large Scale Combustion Chamber

Annular ignition and flameholding without the aid of a hydrogen pilot flame was successfully accomplished in the large scale combustion chamber.

Temperature and Pressure Effects on Combustion Processes

A series of nine runs to find the effect of pressure on flame speed has been made in the range of 7 psia to 22 psia.

Flow Associated with the V-Flame

The work on a potential flow analysis of the confined and unconfined V-flame was furthered.

Detonation

The design of the shock tube was completed and one of the segments was fabricated. Fabrication of other segments was delayed pending a pressure check of the above.

Blow Down Equipment

The design study of the blow down system was continued.

V. Progress

Blowoff Velocities of Flameholders

A portion of this period was devoted to the final assembly of the equipment described in the previous Progress Report.[1] The rotameters used to measure the propane were carefully calibrated with propane, both volumetrically and gravimetrically. Previous experience had indicated that the manufacturers calibration with air and their recommended corrections are not always applicable to propane. The orifice used to meter the air was constructed and then calibrated with air.

While measuring blowoff velocities for spherical flameholders, the pressure of a stable pilot flame was noted at higher jet velocities and ca. stoichiometric mixtures. At lower jet velocities the stable pilot flame was observed only in very rich or very lean mixtures, i.e., just before blowoff occured.[2] Photographs were taken of these typical flames using a 0.125 inch diameter spherical flame holder in a one inch diameter jet. Photograph 7 (Figure 1) shows a flame with a fuel-air ratio of 0.05% at a jet velocity of 186 feet per second, while Photograph 8 (Figure 2) shows a flame with the same fuel-air ratio but at a jet velocity of 268 feet per second. As evidenced by these photographs, it may be seen that at the jet velocity of 186 feet per second (Photograph 7) steady state combustion is maintained far downstream from the holder while at the higher jet velocity (Photograph 8) combustion is confined to a very small region immediately downstream of the spherical flameholder.

From aerodynamic considerations, it seemed that a bluff body located downstream of the spherical flameholder would provide a low velocity region and might again stabilize the flame and allow it to propagate. The effect of the insertion of a cylindrical rod at the critical position into the pilot flame shown in Photograph 8 may be seen in Photograph 9. The jet velocity and fuel-air ratio in Photographs 8 through 14 are exactly the same. The appearance of the flame when the cylinder is below the critical position is shown in Photograph 10. Photographs 11 and 12 show the appearance of the flame as the cylinder is progressively moved downstream from the spherical flame holder. Photograph 13 is a photograph of a smaller diameter

---

1. See Reference 2
2. See Reference 1

cylinder inserted at the critical position in the pilot flame shown in Photograph 8, while Photograph 14 shows the appearance of the flame with the same cylinder inserted further downstream. It appears that there is a variation in the critical distance above the flameholder for a variation in cylinder size, as is shown in Photographs 10 and 13.

Immediately following are Photographs 7, 8, 9, 10, 11, 12, 13, and 14 (Figures 1 through 8, pages 5 through 12).

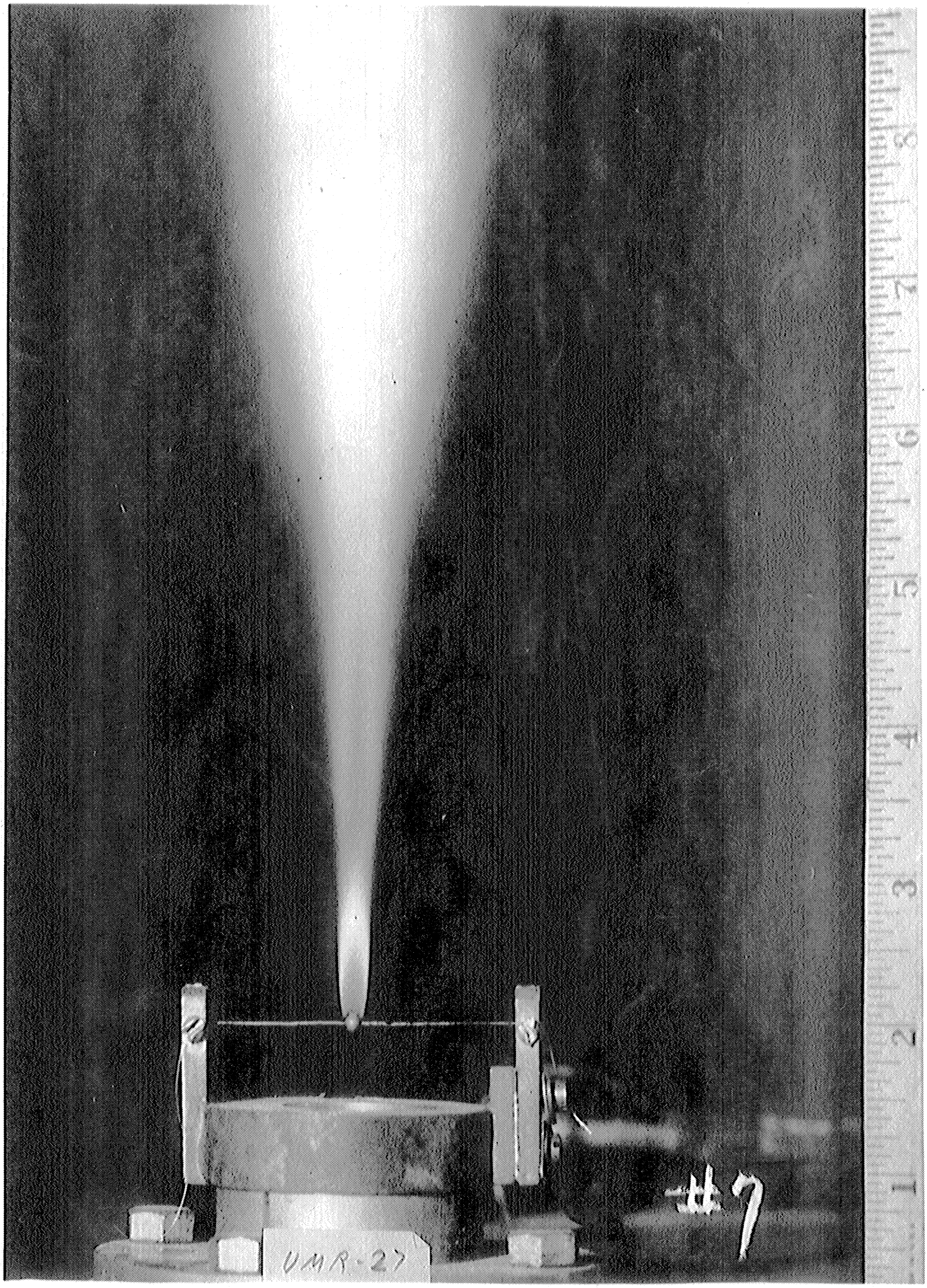
#7
UMR-27

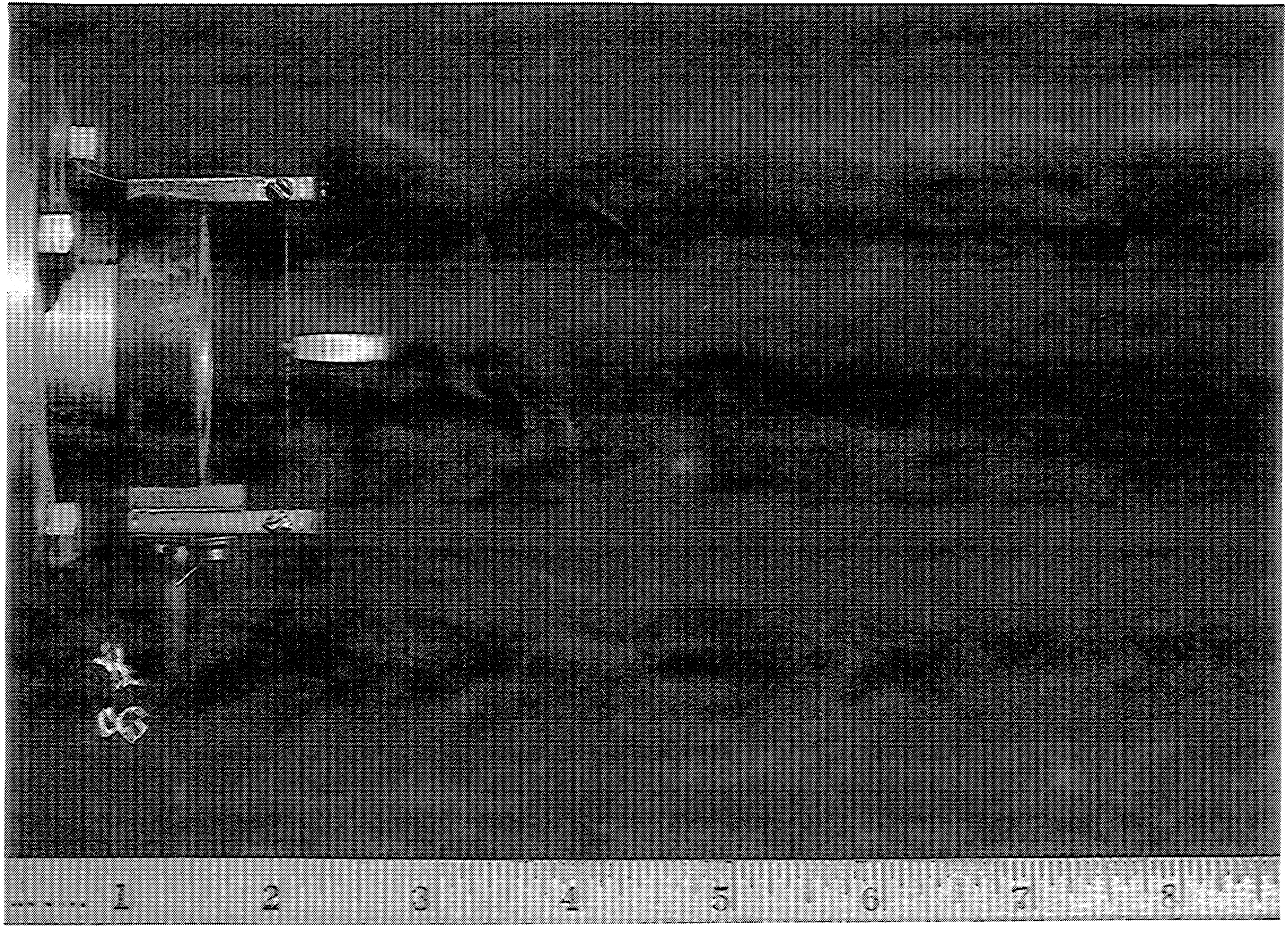
#8
1
2
3
4
5
6
7
8

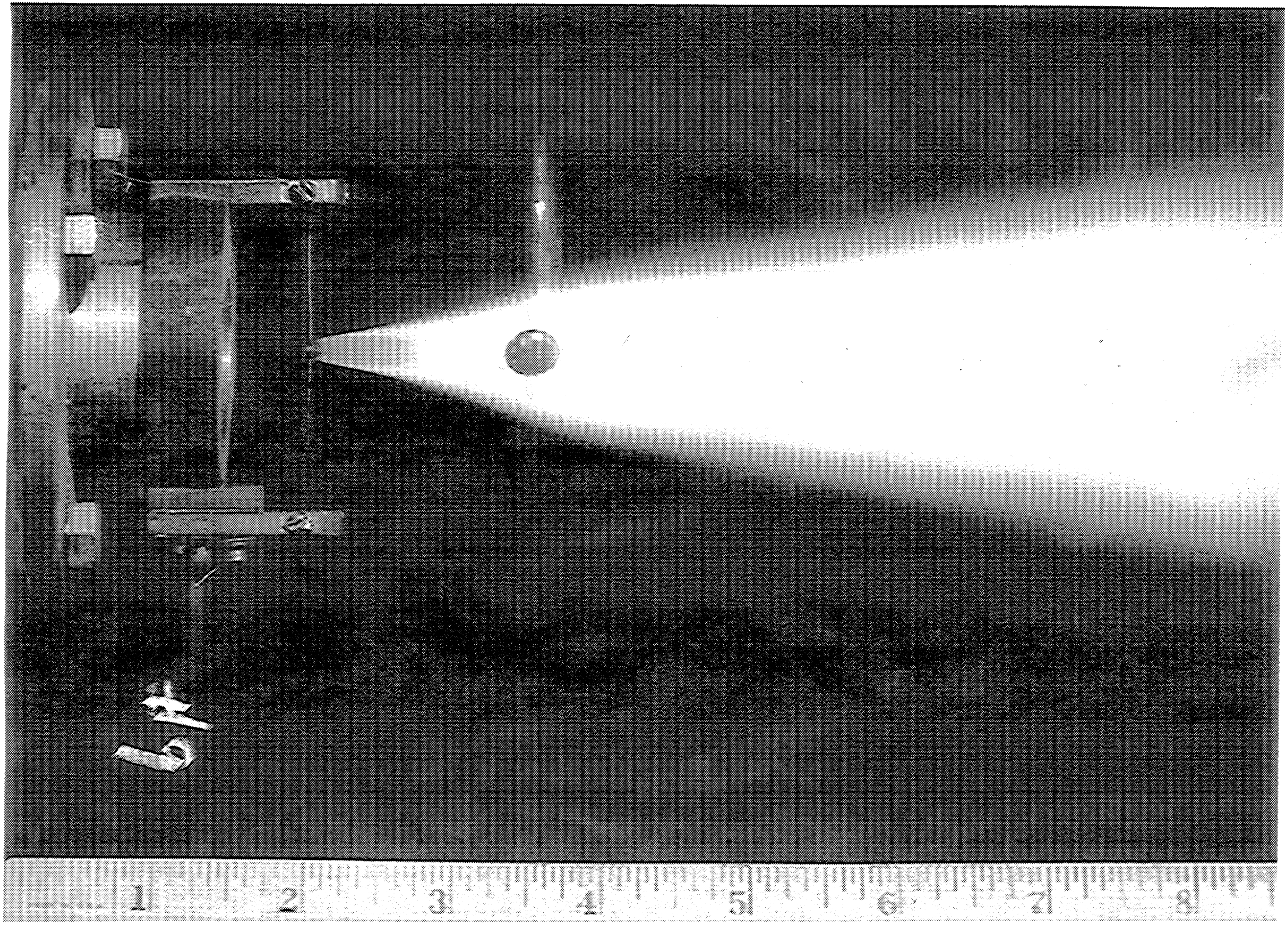
#9
1
2
3
4
5
6
7
8

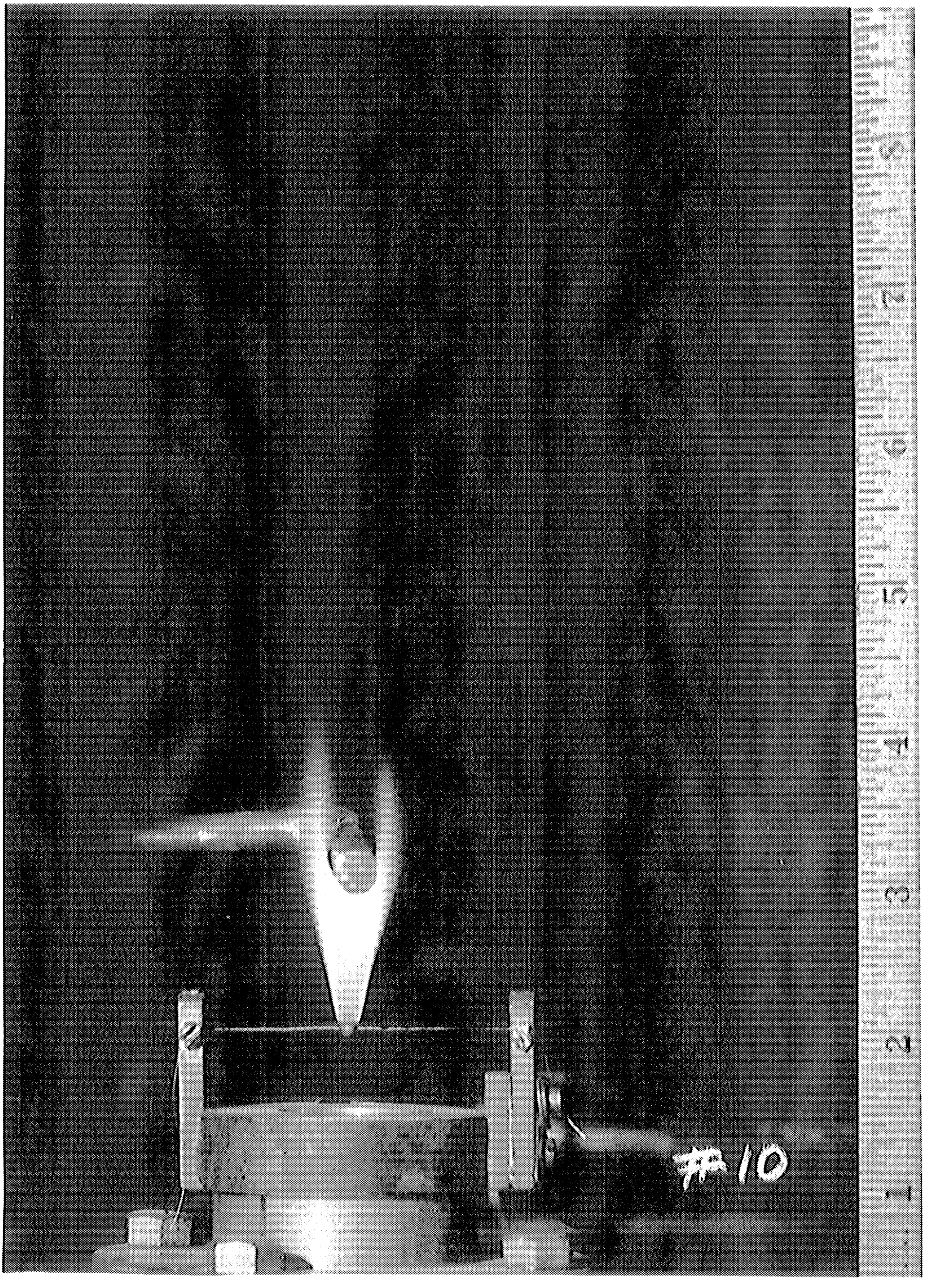
#10
1
2
3
4
5
6
7
8

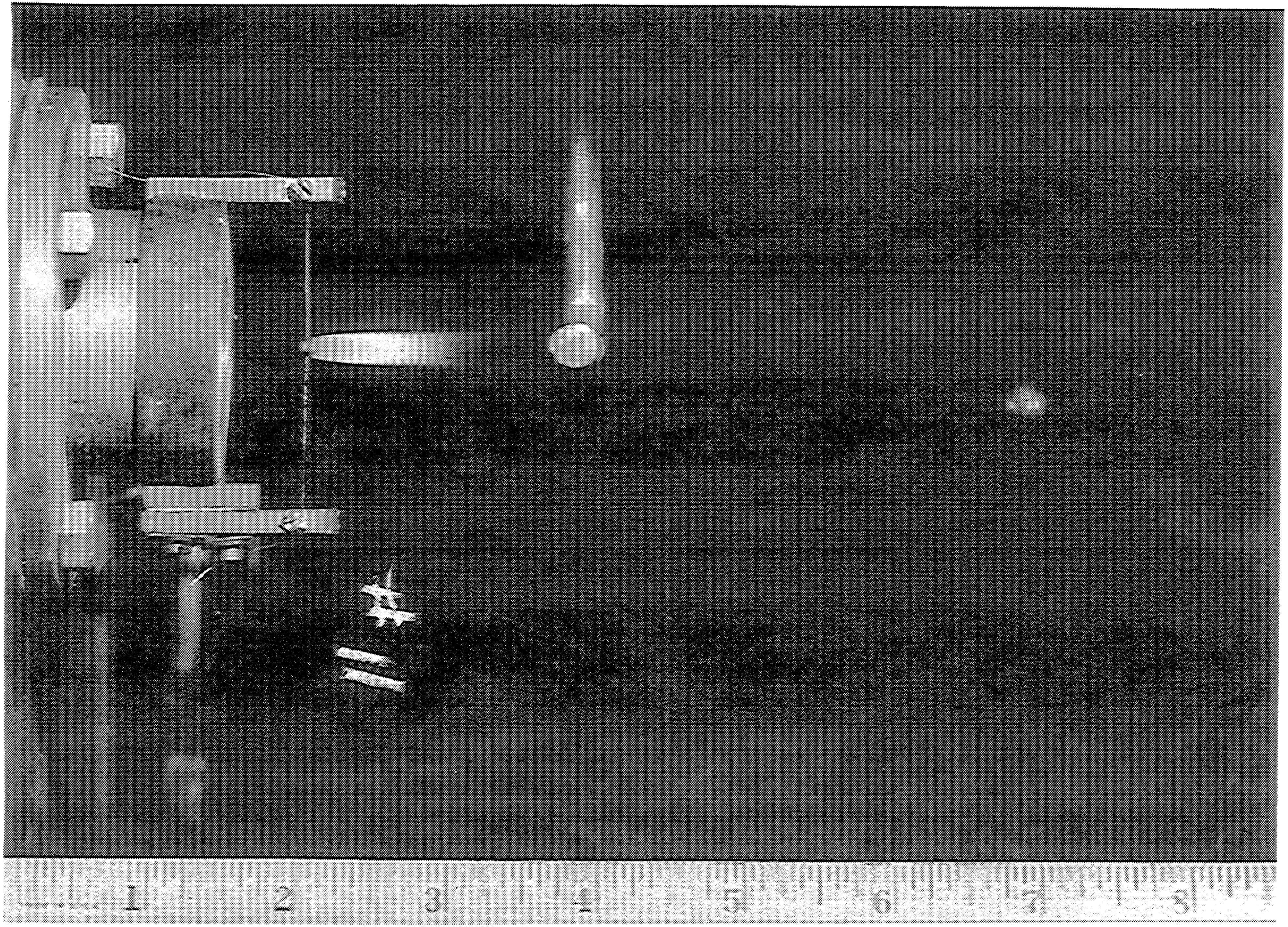
#11
1
2
3
4
5
6
7
8

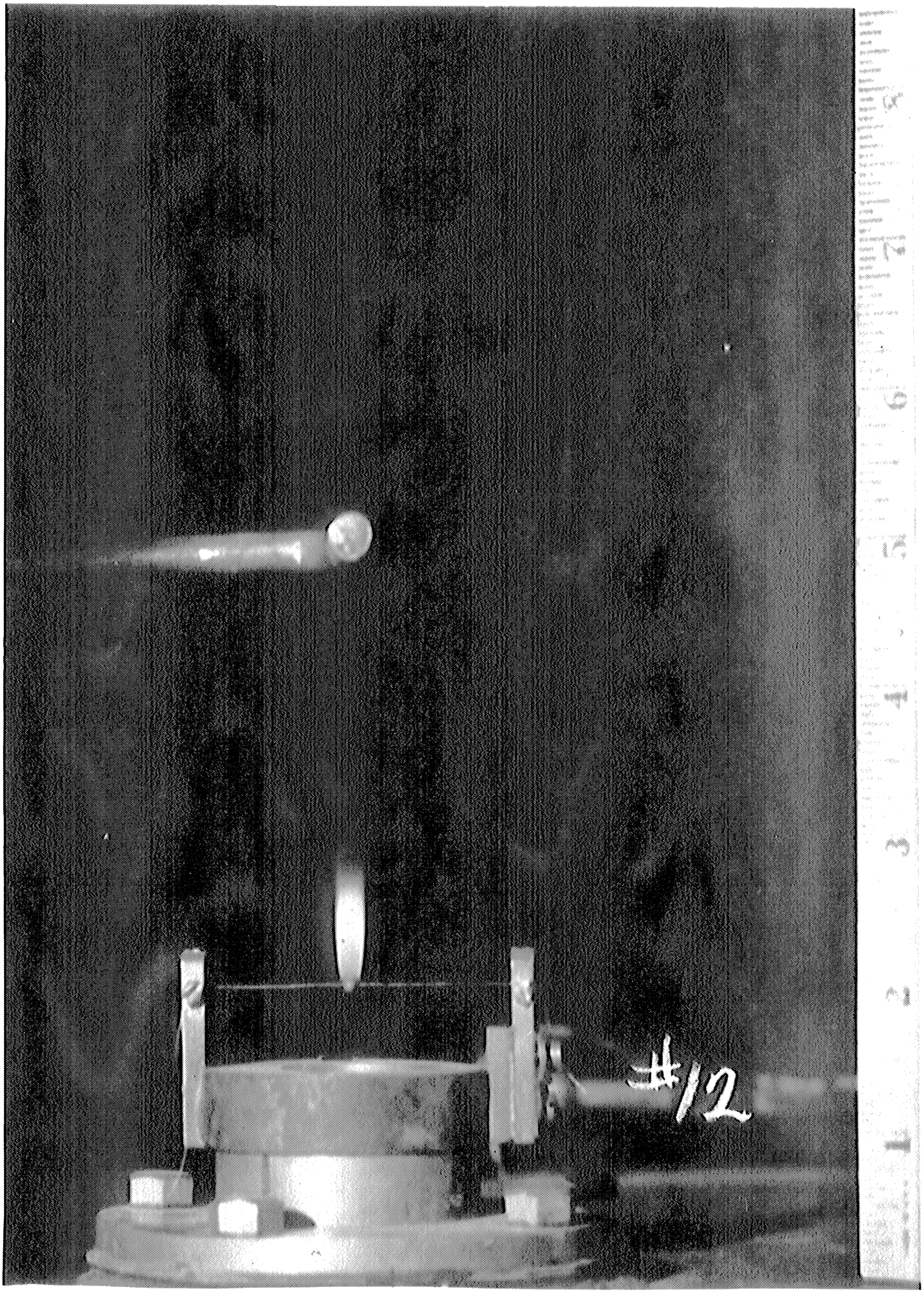
#12

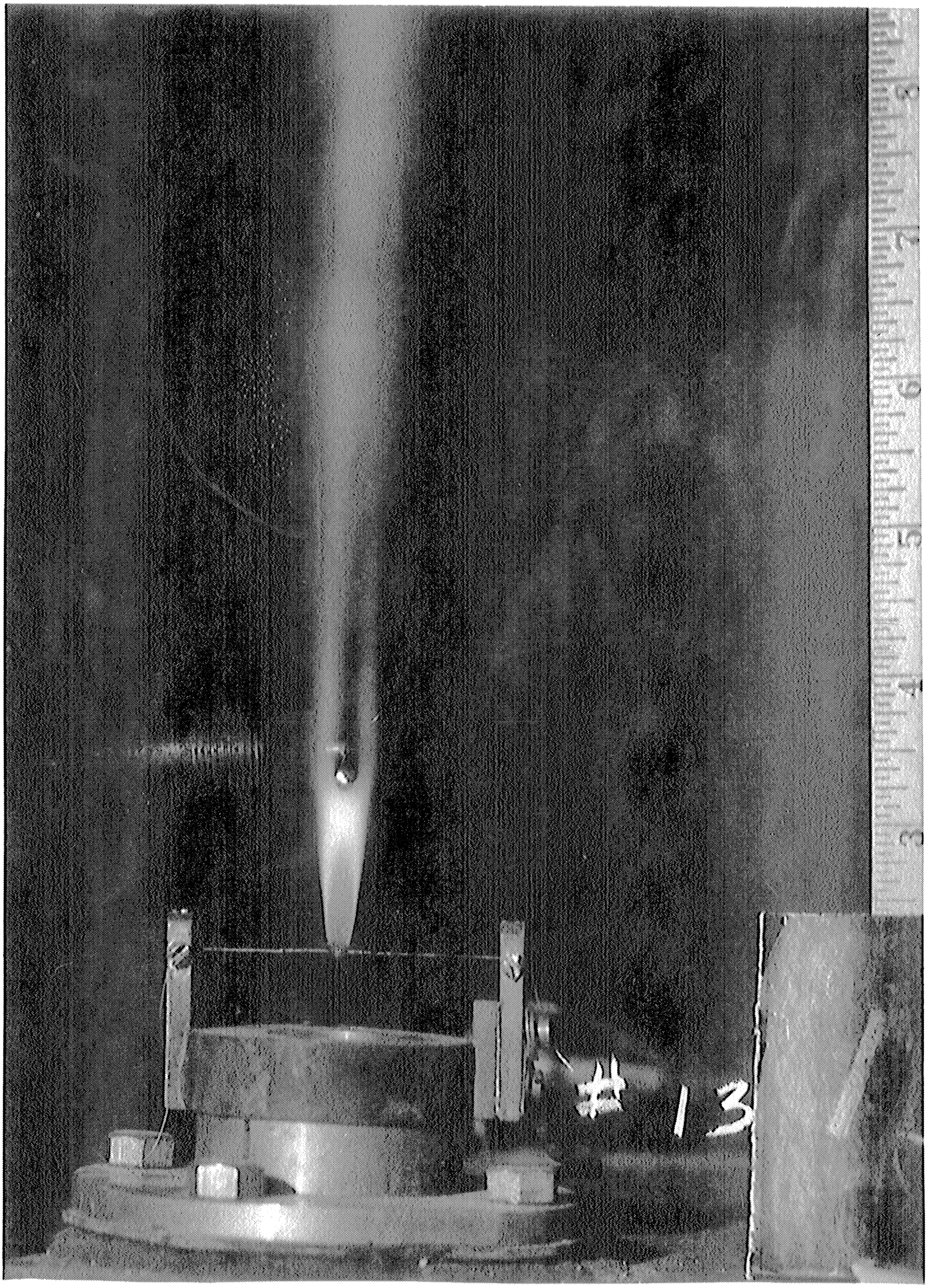
#13

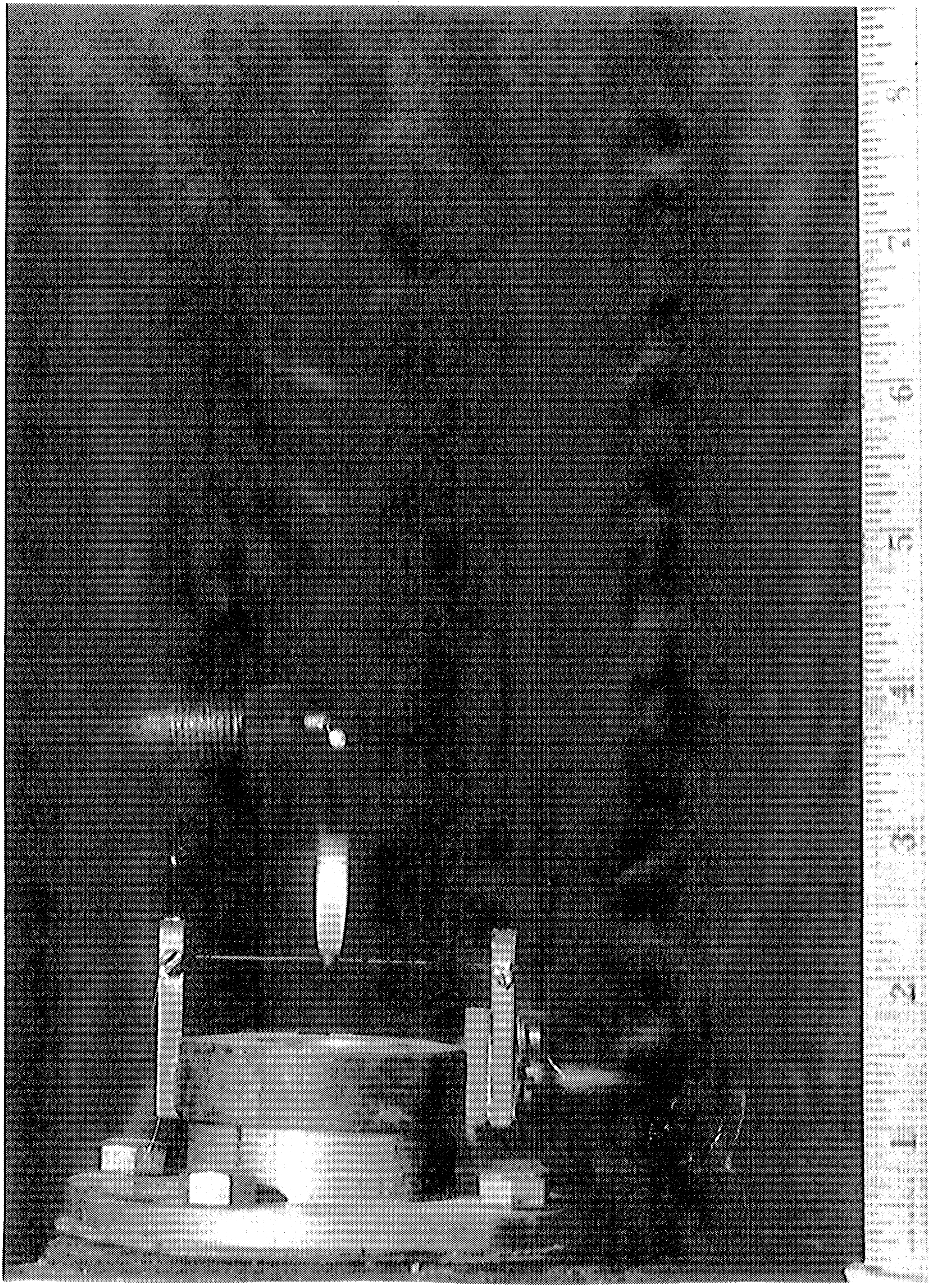
8
7
6
5
4
3
2
1

Large Scale Combustion Chamber

The four inch combustion chamber has been modified to the extent that ignition and flame holding are accomplished with the aid of an annular volume similar to that described in UMC-27 (Reference 4). This modification was made in an effort to obtain a burner that would ignite reliably with gasoline only, so that the use of hydrogen or other gaseous fuel would be unnecessary for future testing. A preliminary simplified annulus and flameholder assembly was installed and satisfactorily operated with 91 Octane aviation grade gasoline at injection pressures up to 300 psi. Ignition was very reliable (two standard I-16 turbo-jet spark plugs provided the spark) and combustion was maintained at inlet air velocities up to 150 feet per second. An improved assembly which will allow better control of the fuel distribution and more flexibility of flameholder design and location is now being fabricated (see Figure 9). The main purpose of the annular volume is to initiate and maintain a combustion zone nearly independent of the flow velocities at the combustion chamber entrance. The propagation of the flame into the main stream is then primarily a problem of flameholder design. It might be better, perhaps, to speak of a "flame propagator" instead of a "flame holder" as the flame will actually be held in the annulus volume.

Temperature and Pressure Effects on Combustion Processes

Due to the many complications in the calibration of the equipment as outlined in the previous progress reports, it was decided to make certain changes in the set-up. A schematic drawing of the present test apparatus is shown in Fig. 10.

In the new set-up a series of steel cylinders was obtained and pressurized to 210 psig with various fuel-air mixtures. The storage tanks were evacuated to a few millimeters of Hg by a water ejector, then flushed with propane and re-evacuated. A different fuel-air ratio was then put in each cylinder by adding propane to the evacuated cylinder up to a certain pressure, then charging with air to a precalculated total pressure. Compressibility of both propane and air was taken into account when filling the cylinders. The fuel-air cylinders are kept above 100°F. during operation by use of steam coils. The cylinders are stored in a small sandbagged building approximately fifty feet from the laboratory. By use of these

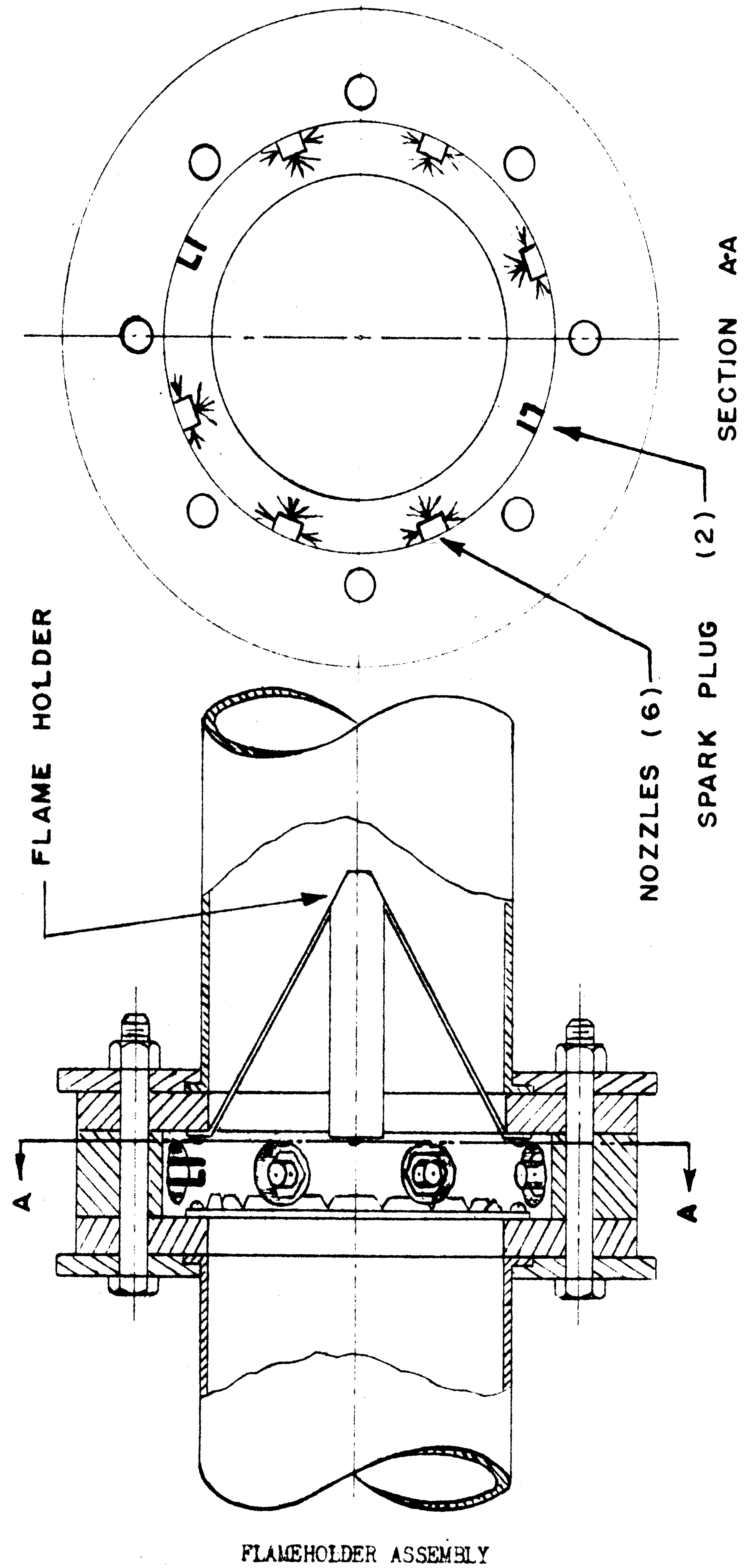

FLAMEHOLDER ASSEMBLY

Figure 9

fuel-air cylinders it was possible to maintain constant fuel-air ratios under varying pressure runs by use of only one control valve. This system also eliminated the use of capillary flow tubes for the measurement of the separate flows and made it possible to use a rotameter for the measurement of the combined flow.

The fuel-air mixture passes through a flash trap to the control valve, then through the rotameter to the Bunsen tube. The rotameter pressure and temperature are recorded and used to calculate the flow of gas to the Bunsen tube. Live steam is fed into the jacket about the Bunsen tube in order to keep condensation off the lip of the Bunsen tube and to keep the lip at a constant temperature, thus eliminating any effect of temperature on flame speed. The desired vacuum in the combustion box is obtained by a balance between the exhaust and ejector valves. At pressures higher than atmospheric, the desired pressure is obtained by a balance between the exhaust and control valves. The combustion box pressure is read from a 100 inch U-tube mercury manometer for vacuum and low pressure runs and from a calibrated bourdon type pressure gauge for high pressure runs. A pressure dampener is used in the lines from the combustion box to the pressure gauges to dampen out all fluctuations of pressure in the combustion box. A secondary air line was installed in the combustion box for future experiments. A one inch blowout flange and diaphragm was installed in the combustion box for safety reasons. During runs the windows in the box are kept clear of condensation by a small radiant electric heater, thus keeping the windows at a temperature above the dew point of the gases in the combustion box.

Photographs are taken of each run. The camera used was a Speed Graflex. The flame was photographed at f-11 and at a shutter speed of one second, thus eliminating the possibility of recording a momentary fluctuation of the flame. The flame speeds are obtained from the photographs by the projection of the cones up to twelve times the normal size. The surface area is then measured and the normal flame speed is computed by the Guoy or Area Method:

$$V_f = \frac{Q}{A_c}$$

where V_f is the normal flame speed relative to the unburned mixture; Q is the volumetric rate of flow of the unburned mixture, and A_c is the surface area of the flame cone.

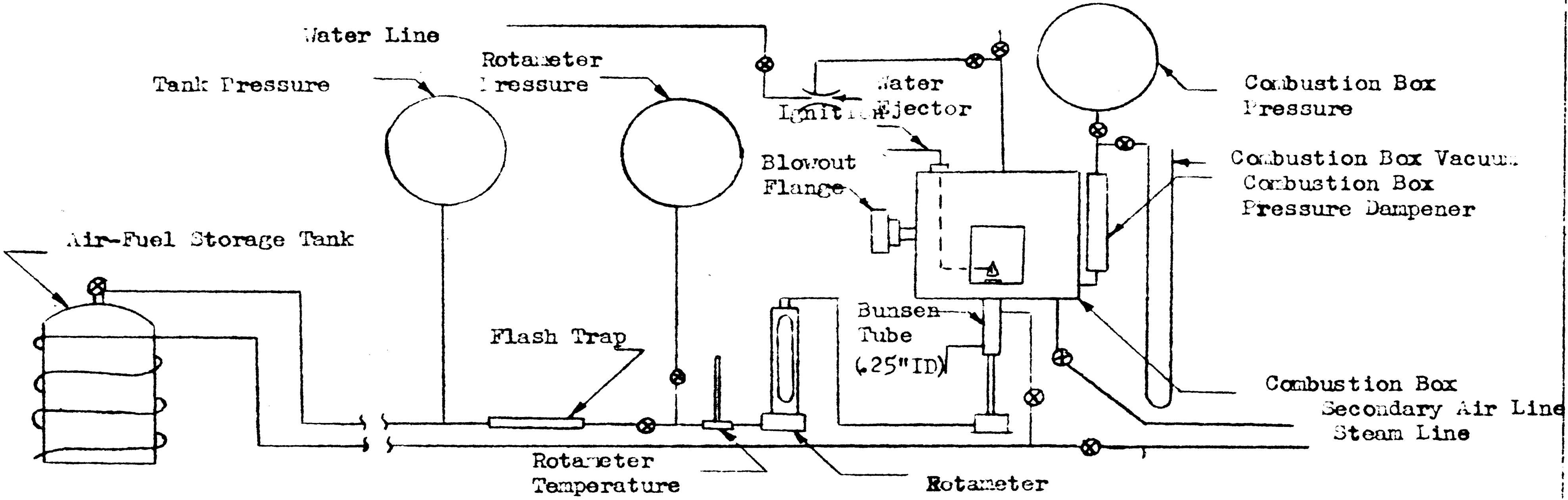

Gas flows from Air-Fuel storage tank, heated by steam coils to the desired temperature, through a flash trap to the flow control valve. From the flow control valve the gas flows through a rotameter and into the Bunsen tube. The temperature of the Bunsen lip is kept constant by a circulation of steam through a jacket about the bunsen tube. The Combustion Box pressure is read from a Mercury U-tube manometer for vacuum and low pressure runs and from a calibrated bourdon type gage for higher pressures. A dampener was installed in this line to dampen out all fluctuations of pressure in the combustion box. The desired combustion pressure is controlled in the box from prpper manipulations of the exhaust and control valves.

Figure 10

Schematic Drawing of Test Set-up to Study Temperature and Pressure Effects on Combustion Processes

Preliminary runs from 1/3 atmosphere to over six atmospheres have been performed to test the equipment. Some interesting phenomena have been observed in the sub-atmospheric runs, one of which is a normal flame as shown in Figure 11 at a pressure of ten inches mercury absolute. A similar Bunsen flame was observed by H.G. Wolfhard and is outlined in his report "Die Eigenschaften stationarer Flammen im Unterdruck". A translation of this report was made by Mr. R.E. Cullen of this group. This translation is being compiled by the Reports Office at the U. of M. Aeronautical Research Center and will be forwarded at an early date.[1]

A series of runs was made at nine fuel-air ratios ranging from .055 to .090. Photographs were taken of the Bunsen flame at the following pressures: 7.76, 11.69, 14.63, 18.56, and 22.00 psia. From these photographs the flame speed, V_f, was obtained as previously outlined. These data are plotted in Figure 12 which indicate that flame speed decreases with increasing pressure. However, there is a reversal in the general trend of this figure for the curve at a pressure of 7.76 psia. Under vacuum the flames become less luminous, thus making it more difficult to establish the exact boundaries of the flame surface. Lower pressures will be studied and a new photographic technique employed during the next period in order to substantiate or disprove this reversal in trend. The photographs of the flames taken at extremely rich mixtures approximate a tetrahedron rather than a cone, thus making computation of the flame surface with one picture extremely difficult. The points obtained at a fuel-air ratio of .090 were not included in the plot for this reason.

In comparison with the report by H.G. Wolfhard, as previously mentioned in this section, some disagreement occurred. Wolfhard used stoichiometric mixtures of acetylene and oxygen and acetylene and air. He observed that the flame speed was practically constant between pressures of 10 mm and 760 mm Hg absolute pressure. The only apparent difference between the methods employed by Wolfhard and those used here is that he did not state that the burner lip was kept at a constant temperature as was done here. Previous work done by Mr. R.B. Morrison and Mr. R.A. Dunlap at this facility has shown that this temperature apparently affects flame speeds. This characteristic is outlined in report UMM-21.[2] Possibly, another reason for the disagreement in the trend of the curves might be due to the difference in fuels used. To check this discrepancy, various fuels will be used at a later date.

An interesting phenomenon was observed which is incidental to the effect of pressure on flame speed. This was the variation of the distance, δ_Q, between the burner lip and the bottom of the flame. A plot of δ_Q with pressure for two fuel-air ratios is given in Figure 13.

---

1. See Reference 3.
2. " " 5.

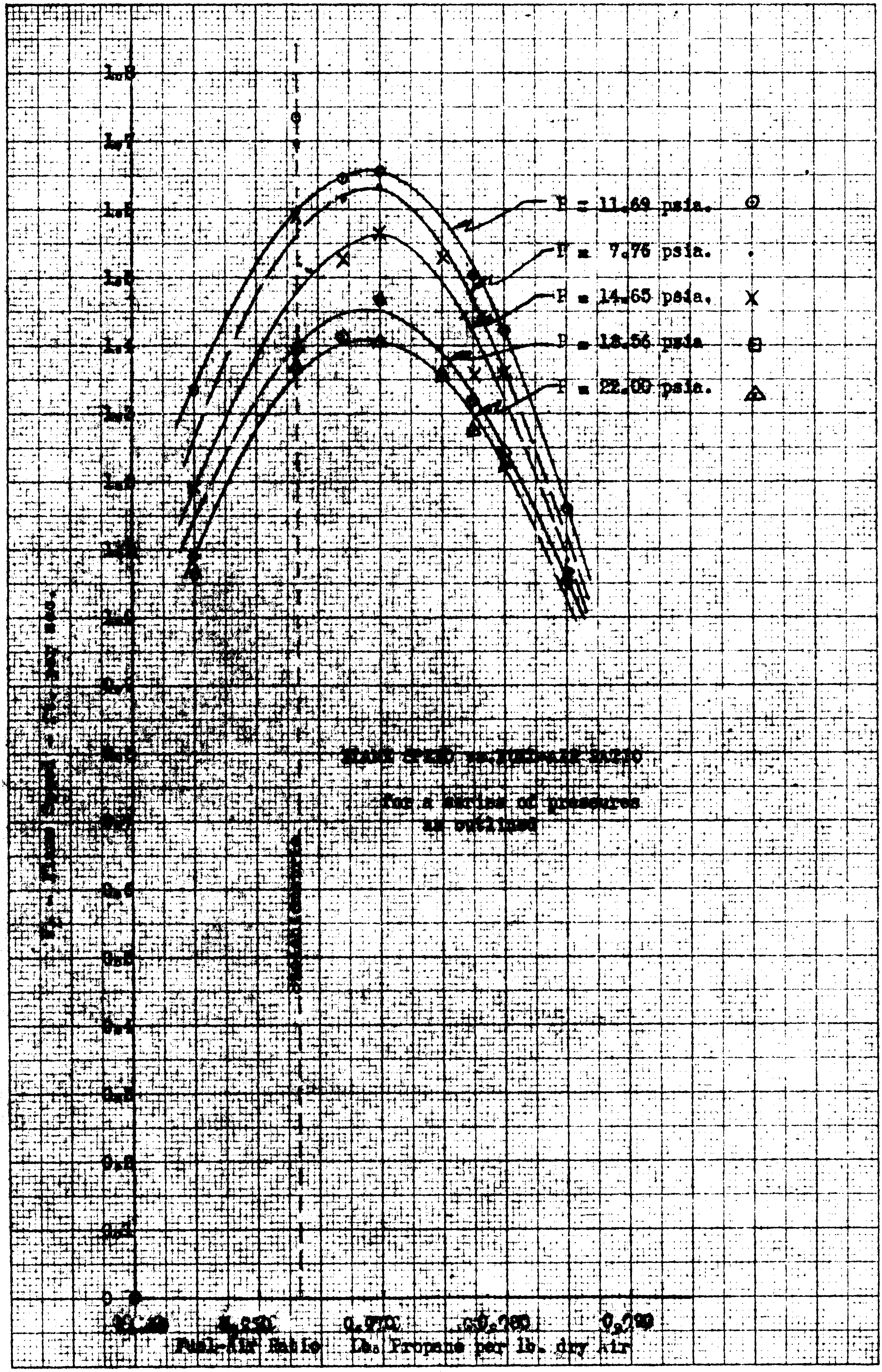
1.8
1.7
1.6
1.5
1.4
1.2
1.1
1.0
0.9
0.8
0.7
0.6
0.5
0.4
0.3
0.2
0.1
0
P = 11.69 psia. ⊖
P = 7.76 psia. •
P = 14.65 psia. X
P = 18.56 psia ⊟
P = 22.00 psia. △
For a series of pressures
as outlined
0.080
Fuel-Air Ratio Lbs. Propane per lb. dry Air

Fig. 12

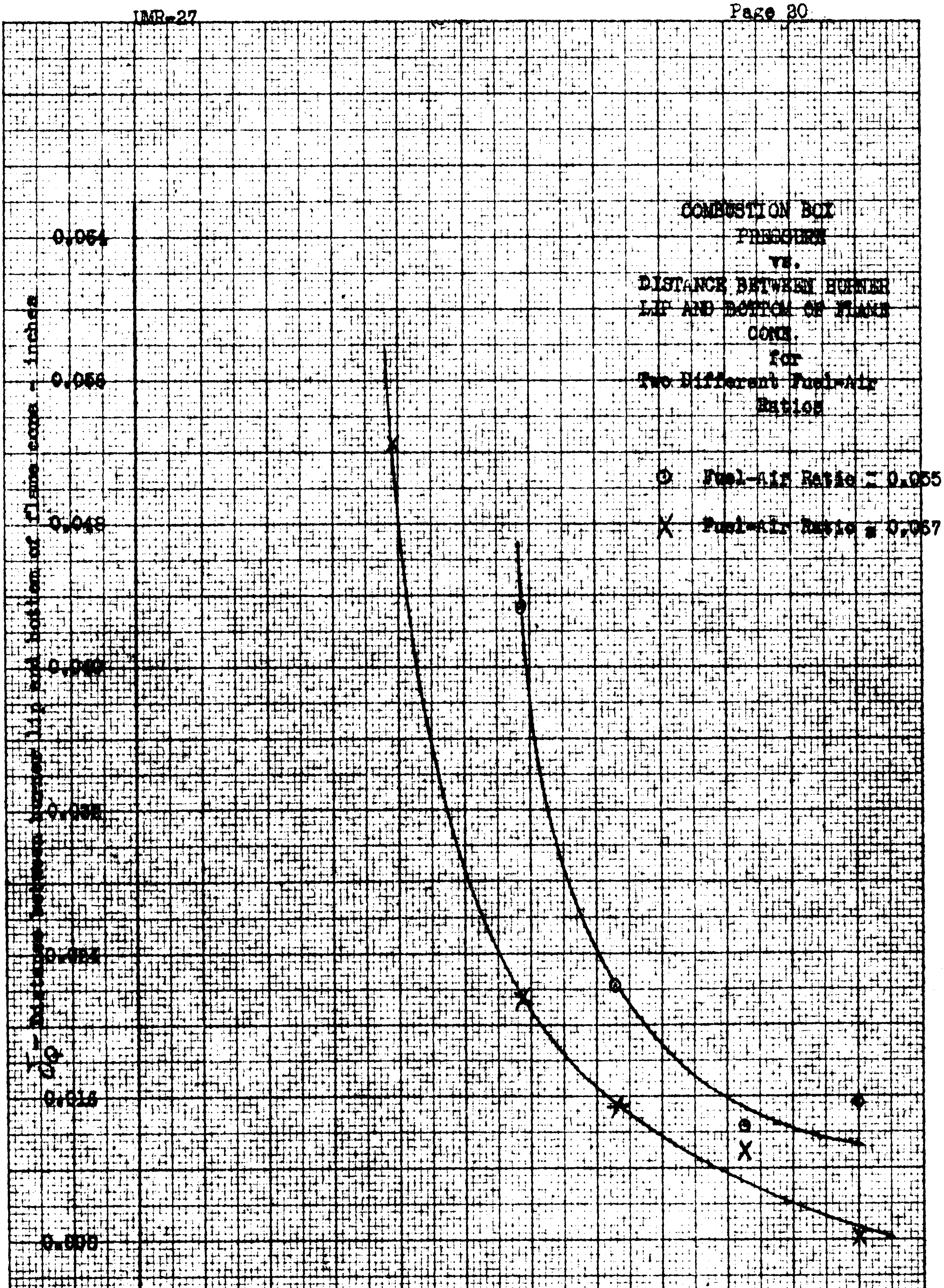
COMBUSTION BOX
PRESSURE
vs.
DISTANCE BETWEEN BURNER
LIP AND BOTTOM OF FLAME
CONE
for
Two Different Fuel-Air
Ratios
○ Fuel-Air Ratio = 0.055
X Fuel-Air Ratio = 0.067
Distance between burner lip and bottom of flame cone - inches
0.064
0.056
0.048
0.040
0.032
0.024
0.016
0.008
0.000
0
2
4
6
8
10
12
14
16
18
20
22
Pressure - psia.

Fig. 13

V-Flame Analysis

In the past two periods a mathematical analysis of the gas flow associated with a V-flame has been attempted. This analysis has been made for both the unconfined and the confined V-flame. A summary is given here of the different types of approaches to the solution of these two problems and their results.

The Unconfined Two-Dimensional V-Flame

The unconfined two-dimensional V-flame can be defined as a stationary, wedged shaped flame burning in a jet of combustible mixture in which the burning is restricted in one dimension. Such a flame has a stream pattern such as shown in Figure 14. The analysis of this flow can be separated into two parts, the flow from the nozzle to the flame front and flow from the flame front to the surrounding atmospheric air.

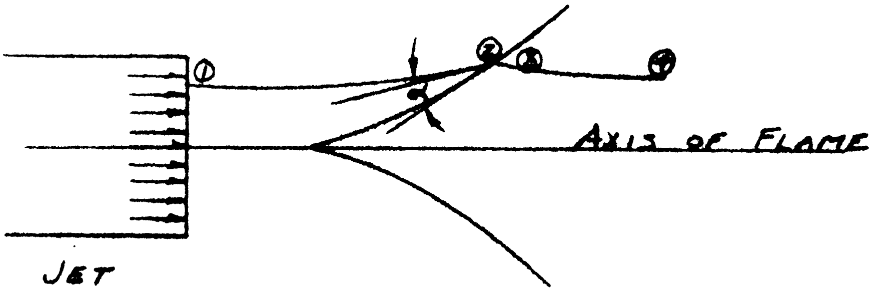

Figure 14

The simplest and most obvious way to analytically describe the flow is through the use of the three fundamental equations of motion, i.e., conservation of mass, momentum, energy and the equation of state. The flow up to the front would utilize the conservation of mass and energy; the flow across the front, the conservation of mass, momentum and energy, and the flow away from the front, the conservation of mass and energy. Assuming a perfect fluid, these conditions yield:

$$\left.\begin{array}{l} P_1 + \tfrac{1}{2}\rho_1 V_1^2 = P_2 + \tfrac{1}{2}\rho_2 V_2^2 \\ \rho_1 A_1 V_1 = \text{CONST.} \end{array}\right\}$$

....Energy equation for isentropic steady flow (1)

$$\left.\begin{array}{l} P_2 + \rho_2 V_2^2 = P_3 + \rho_3 V_3^2 \\ \rho_2 A_2 V_2 = \rho_3 A_3 V_3 \\ h_2 + \tfrac{1}{2} V_2^2 + Q = h_3 + \tfrac{1}{2} V_3^2 \end{array}\right\}$$

..................(2)

$$\left.\begin{array}{l} P_3 + \tfrac{1}{2}\rho_3 V_3^2 = P_4 + \tfrac{1}{2}\rho_4 V_4^2 \\ \rho_3 A_3 V_3 = \text{CONST.} \end{array}\right\}$$

..................(3)

The problem is then to solve these equations given the flame angle, β_3, and the nozzle exit conditions to give velocities, pressures, etc., along a streamline. Any combination of these equations, however, seems to lead to expressions such as:

$$\frac{\rho_3}{\rho_1} = \frac{V_1^2 + V_2^2}{V_3^2 - V_4^2} = \frac{V_1^2 + V_2^2}{V_4^2 + V_2^2 + V_2^2 \sin^2\alpha\left[\left(\frac{\rho_3}{\rho_1}\right)^2 - 1\right]} \qquad (4)$$

which has two unknowns, i.e., one dependent and two independent variables which cannot be determined without knowing the actual streamline pattern or without being able to measure certain velocities or their corresponding pressures. The latter would be difficult to do experimentally due to the small magnitude of the pressure changes.[1] While this analysis does not allow quantitative results without experimental measurements, it does allow a qualitative description of the flow field such as was given in Progress Report UMR-23.

Another attempt was made to describe the flow by solving the differential equations for irrotational incompressible flow. These equations are the Cauchy-Rieman equations, namely: (the coordinate system is shown in Figure 15)

$$\frac{\partial u}{\partial y} - \frac{\partial v}{\partial x} = 0 \qquad \text{condition for irrotational flow} \qquad (5)$$

$$\frac{\partial u}{\partial x} + \frac{\partial v}{\partial y} = 0 \qquad \text{conservation of mass} \qquad (6)$$

These two conditions are satisfied by LaPlace's equation which in terms of the stream function is:

$$\frac{\partial^2 \psi}{\partial x^2} + \frac{\partial^2 \psi}{\partial y^2} = 0 \qquad (7)$$

One of the methods for solving this equation, which often succeeds in physical problems, is to assume that ψ can be written as:

$$\psi = X(x) \cdot Y(y) \qquad (8)$$

---

[1] The pressure rise from the nozzle to a propane flame is in the order of .00001265 atm.

La Place's equation then becomes

$$\frac{1}{X}\frac{\partial^2 X}{\partial x^2}+\frac{1}{Y}\frac{\partial^2 Y}{\partial y^2}=0 \qquad (9)$$

which can be separated into

$$\frac{1}{X}\frac{\partial^2 X}{\partial x^2}=\pm a^2 \qquad \text{and} \qquad \frac{1}{Y}\frac{\partial^2 Y}{\partial y^2}=\mp a^2$$

for which possible solutions are:

$$\begin{aligned}\psi = {} & C_1 e^{ay}\cos ax,\ C_2 e^{ay}\sin ax,\ C_3 e^{-ay}\cos ax,\ C_4 e^{-ay}\sin ax,\\ & C_5 e^{ax}\cos ay,\ C_6 e^{ax}\sin ay,\ C_7 e^{-ax}\cos ay,\ C_8 e^{-ax}\sin ay\\ & C_9 x,\ C_{10} y,\ C_{11} xy,\ C_{12}\end{aligned}$$

The boundary conditions which can be applied to this problem are:

(1) $\psi = 0$ when $y = 0$

(2) $v = 0$ when $x = -\infty$

(3) $u = V_1$ when $x = -\infty$ Where V_1 is the uniform jet velocity shown in Figure 15 .

The first boundary condition eliminates all solutions except

$$\psi = C_6 e^{ax}\sin ay,\ C_7 e^{-ax}\sin ay,\ C_{10}\, y,\ C_{11}\, xy$$

The second boundary condition eliminates all solutions except $\psi = C_{10}\, y$, $\psi = C_6 e^{ax}\sin ay$ when a is assumed to be a positive number. The third boundary condition demands $C_{10} = V_j$, or finally:

$$\psi = C_6 e^{ax}\sin ay + V_1 y \qquad (10)$$

$$u = aC_6 e^{ax} \cos ay + V_1 \qquad (11)$$

$$v = -aC_6 e^{ax} \sin ay \qquad (12)$$

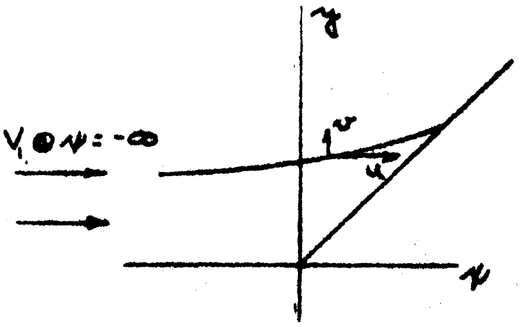

Coordinate System
Figure 15

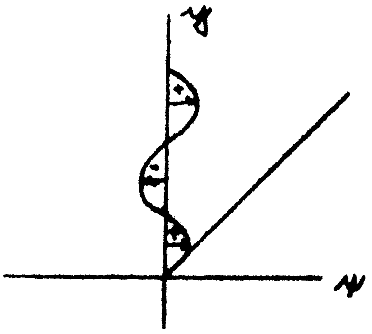

v - Velocity Profile
Figure
16

These equations describe a potential flow and might apply to flow up to the flame front. Inspection of these equations show, however, that the v component of velocity is a cyclic function of y, i.e., for constant x, v will vary as sin (ay) and will, for a finite value of a different from 0, give a velocity profile such as is shown in Figure 16. This indicates that at some distance from the axis of the flame the stream will alternately diverge and converge which is contrary to any experimental data so far accumulated on the unconfined V-flame. On the basis of the above, it is concluded that equations (10), (11), and (12) do not represent the actual flow pattern, the reason probably being that the original assumption for the form of the solution (equation 8) is not the one which represents the actual case. It is not immediately obvious what assumption would be necessary to represent the flow.

A third analysis of this problem, made by the Mathematics Group at the Research Center, is presented in EMV-3 and is reviewed briefly here. In this report, solution to the problem is attempted by adding two complex potential functions, one representing a uniform flow parallel to the axis of the flame and a second representing flow around a corner, i.e., $W = Z + Z^n$, yielding:

$$\Phi = \phi_1 + \phi_2 = Ur^n \cos n\theta + C_1 Ur \cos\theta + C_3 \qquad (13)$$

$$\Psi = \Psi_1 + \Psi_2 = Ur^n \sin n\theta + C_1 Ur \sin\theta + C_4 \qquad (14)$$

$$u = u_1 + u_2 = nUr^{n-1}\cos(n-1)\theta + C_1 U \quad (15)$$

$$v = v_1 + v_2 = v_1 + 0 = nUr^{n-1}\sin(n-1)\theta \quad (16)$$

Where θ, r are measured as indicated in Figure 17 and u and v are the velocity components parallel and perpendicular to the axis of the flame respectively, $U = \frac{V_1}{\left(\frac{\pi}{\theta'} - C_1\right)}$, $\theta' = \frac{\pi - \text{FLAME} \measuredangle}{2}$, $n = \frac{\pi}{\theta'}$

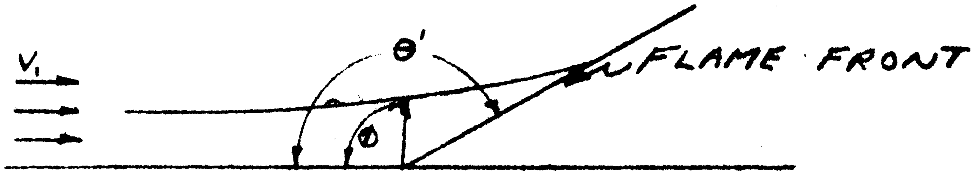

Figure 17

This solution, however, does not satisfy the boundary condition on page that $u = V_1$ when $\psi = -\infty$ or in terms of polar coordinates $u = V_1$ when $\theta = 0, r = \infty$. This fact is seen from equation (15) which, when evaluated for this boundary condition, becomes:

$$u = \frac{\pi}{\theta'} U \infty^{\pi/\theta' - 1} \cos\left(\frac{\pi}{\theta'} - 1\right) \cdot 0 + C_1 U$$

and since $\pi/\theta' \neq 1$, $u = \infty \neq V_1$

Since the solution does not satisfy the boundary condition imposed, it does not represent the actual flow pattern. The process of finding the correct complex function seems to be one of trial and error and so this type of analysis was discontinued.

The Confined Two-Dimension V-Flame

The confined V-flame is defined as a flame burning as a wedge in a combustion chamber with parallel walls such as shown in Figure The analysis of the flow associated with this flame has proceeded in the same manner as for the unconfined V-flame analysis.

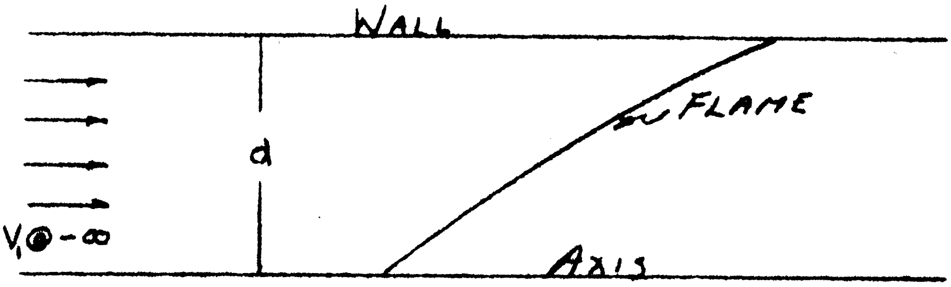

Figure 18

The results have been more useful, however, in that the confined flame allows another boundary condition which makes the analysis of page 22 useful. The boundary conditions on the confined flame are the three of the unconfined flame plus a fourth $v = 0$ at $y = d$ (Figure18). Applying this fourth boundary condition to equation (12) and restricting the solution for v to the first $\frac{1}{2}$ cycle in Figure 16, gives

$a = \frac{\pi}{d}$. Equations (10), (11), and (12) then become:

$$\psi = c_6 e^{\frac{\pi}{d}x} \sin \frac{\pi}{d} y + V_1 y \tag{10a}$$

$$u = \frac{\pi}{d} c_6 e^{\frac{\pi}{d}x} \cos \frac{\pi}{d} y + V_1 \tag{11a}$$

$$v = -\frac{\pi}{d} c_6 e^{\frac{\pi}{d}x} \sin \frac{\pi}{d} y \tag{12a}$$

This equation now satisfies all boundary conditions known on the confined V-flame. The solution has one undetermined constant, c_6, which could be determined experimentally; however, it would not be necessary to determine the constant to determine velocity gradients, variation of flame speed along the flame front, etc. which at this time seems to be important.

Detonation

The preliminary phase of the theoretical studies of the shock tube and of detonation waves has been completed. A separate report (EMG-14) which presents the details has been prepared and is being edited for publication.

The experimental study has, so far, included the design of the shock tube and shock tube mount. The mount has been fabricated and installed. One shock tube section has been fabricated and is undergoing pressure tests.

Blow Down Equipment

Selection of the heat exchanger materials and several design calculations utilizing these materials have been made. The heat exchanger is to be a pebble bed type, using mullite pebbles (72% Al_2O_3, 28% SiO_2) approximately 3/8" in diameter. The shell is to be lined with Babcock and Wilcox K-26 insulating brick treated with water glass for abrasion resistance. Based upon data from Löf and Hawley,[1] graphs of bed dimensions and cost versus bed diameter for different weight flows of air, and air and bed temperature versus distance through the bed for parameters of running time have been included. It is believed that these data represent optimistic solutions of the heat exchanger problem; a factor of two may be in order. (Figs. 19 & 20)

A fairly rigorous test of the thermal shock resistance of the insulating firebrick has been made. The surfaces of several test sections of brick were coated with water glass in varying amounts to increase their abrasion resistance; the abrasion resistance of the untreated brick is negligible. The bricks were then heated in a controlled furnace to a uniform 2000°F throughout. Next the treated faces of the heated bricks were quenched suddenly in water at room temperature to a depth of approximately ½ inch and held until cool. Four repetitions of this test were made. No spalling of any of the faces of the brick was seen, the heavily coated surfaces having apparently the same thermal shock resistance as those coated more lightly. The abrasion resistance of the heavily coated surfaces was best however. It is believed that the test is more rigorous than actual operating conditions will impose.

Mullite was chosen as the bed material because of the high temperatures required in the heat exchanger and the low cost desired. Since mullite pebbles have a high heat capacity and surface area per

[1] See Reference 10

unit volume of pebble bed, a fairly compact exchanger unit may be built. The exchanger is expected to produce temperatures considerably in excess of those temperatures required in the system.

Pressure regulating valve sizes have been calculated together with line sizes upstream and downstream of the valve. Allowance was made to prevent choking of the flow anywhere in the lines. Correspondence has been carried out with valve manufacturers and one bid has been received to date.

Work has been going forward on the design of a pilot blow down system, utilizing low pressure storage tanks (300 psia), low pressure heat exchanger (300 psia) and a small ($\frac{1}{4}$ inch^2) nozzle area. The purpose of the pilot system is to test thoroughly the performance of the heat exchanger, thereby eliminating as many "bugs" in the design as possible. It is possible that there may be spalling of the firebrick liner and the mullite pebbles. The practical design of the heat exchanger shell, which requires adequate provision for loading the mullite, supporting it, heating, sealing, and unloading it must be done. Coupled with these are the problems of fuel injection downstream of the heat exchanger and proper test section design. Since the pilot system is to be used also for the study of aero-thermodynamic phenomena, it is believed that its construction is justified. Several tanks have been hydraulically tested to date; the location of tanks with a higher working pressure is being attempted since the tanks tested proved inadequate.

ACTIVITIES VISITED

Activities Visited	Subjects Discussed
Westinghouse Research Laboratories Pittsburg, Pennsylvania	Effects of temperature and pressure on combustion processes and flame stability

VII. Program for Next Period

Blowoff Velocities

It is planned to investigate further this apparent interaction of flameholder and downstream bodies in the hope that it will assist in a better understanding of the flame stabilization mechanism and its possible application to extending the blowoff limits of flameholders. Shadowgraph equipment which is under construction at present will be used to assist in the establishment of a logical experimental program to investigate this particular aspect of the problem.

Large Scale Combustion Chamber

The work on the combustion chamber design will continue in an effort to obtain a basic burner which can be used to test some of the variables involved in combustion. Among these variables is fuel injection pressure, which can be varied up to 2500 psi with present equipment. The drag measuring equipment to be used in evaluating combustion efficiency will be installed upon completion of its fabrication. A short section of Pyrex 4 inch glass tubing will be installed just upstream of the flame holder section so that the flame pattern as well as the fuel spray pattern can be observed.

Temperature and Pressure Effects on Combustion Processes

It is planned to continue the pressure studies as outlined in this report to cover a larger range of combustion pressures. An investigation will be made concerning the variation of the distance between the burner lip and the bottom of the flame as affected by combustion box pressure. A new method of photography will be used.

Flow Associated with V-Flame

Fabrication of the confined combustion chamber will be completed as soon as the Vycor glas is obtained for the windows. Upon completion of the combustion chamber, the validity of the solution for flow in the chamber will be checked by observing streamline flow patterns.

Detonation

The report presenting the preliminary theoretical results will be released. The shock tube will be fabricated, assembled and tested. Further theoretical work will be carried out and shock tube experiments initiated.

Blow Down Equipment

It is planned to continue the design study of the large scale Blow Down equipment as well as the pilot equipment. Pending approval, actual construction of the pilot system will be initiated.

References

1) Progress Report No. 1 -- UMR-21 -- University of Michigan
AAF Contract W33-038 ac-21100

2) Progress Report No. 2 -- UMR-25 -- University of Michigan
AAF Contract W33-038 ac-21100

3) Wolfhard, H.G., "Zeitschrift fur Technische Physik", Volume
23-24, 1942-43, page 206.

4) UAC-2M Project Meteor, MIT Meteor UAC-27, "Summary of Experimental
Ram-Jet Burner Research", W.J. Olewinski, October, 1948
(Dates covered April, 1947 to October, 1947).

5) UMM-21 University of Michigan, "The V-Flame as a Method of
Measuring Flame Speed".

6) EMV-3 University of Michigan, "Flow Through a Flame Which has
the Shape of an Isosceles Wedge".

7) Solkolnikoff and Solkolnikoff, "Higher Mathematics for Engineers
and Physicists".

8) Durand, "Aerodynamic Theory", Vol. 1.

9) MIT-Meteor-19 "Flame Stabilization and Propagation on High
Velocity Gas Stream".

DISTRIBUTION

7 Black and White Copies

1 Tracing (Opaque ribbon)

TO: Commanding General
Air Materiel Command
Wright-Paterson Air Force Base
Dayton, Ohio